Nanoscale

Accepted Manuscript

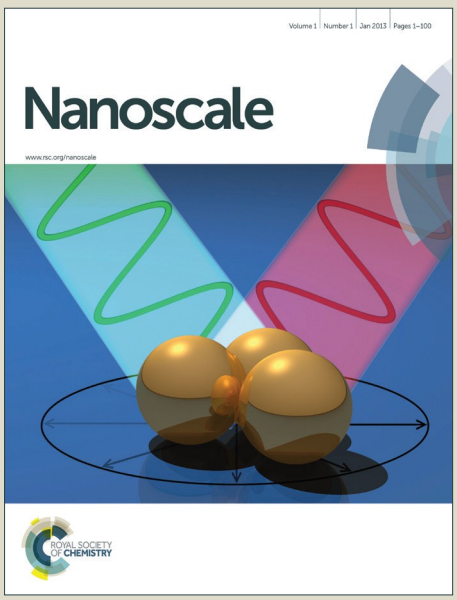

ROYAL SOCIETY OF CHEMISTRY

www.rsc.org/nanoscale

NANOSCALE

RSCPublishing

ARTICLE

Pressure-dependent optical behaviors of colloidal CdSe nanoplatelets

Cite this: DOI: 10.1039/x0xx00000x

Bo Zhou,[a] Guanjun Xiao,[a] Xinyi Yang,[a] Quanjun Li,[a] Kai Wang*[a] and Yingnan Wang*[a]

Received 00th January 2012,
Accepted 00th January 2012

DOI: 10.1039/x0xx00000x

www.rsc.org/

Two-dimensional (2D) colloidal anisotropic CdSe nanoplatelets (NPLs) have attracted a great deal of attraction within recent years. Their strong thickness-dependent absorption and emission spectra exhibit a significant difference with other shaped CdSe nanocrystals (NCs) due to the unique atomically flat morphology. Based on their dielectric confinement effect and the large confinement energy, the 2D CdSe NPLs exhibit the best characteristics of optical and electronic properties as compared to the other CdSe nanocrystallites ensembles. Here, we systematically investigate the *in situ* high-pressure photoluminescence (PL), absorption, and time-resolved PL spectroscopy of CdSe NPLs with different thicknesses. The pressure depended optical behaviors of these NPLs exhibit several remarkable difference comparing with other shaped CdSe NCs, such as the higher phase transition pressure, the irreversible PL and absorption spectra after releasing pressure, the narrower tuneable-range of absorption and PL peak energies, and minor change ranges of PL decay time with increasing pressure. These phenomena and results are attributed to their unique geometric shape and distinctive soft ligand bonding on the surface.

Introduction

Semiconductor nanocrystals (NCs) have attracted a great deal of attention because of their unique physical and chemical properties and potential applications in nanodevices. It is well-known that these properties are greatly influenced by the shape, size, composition and crystal structure of NCs.[1-5] Among these numerous nanostructures, two-dimensional (2D) colloidal anisotropic nanoplatelets (NPLs), especially those with thin thickness (<5 nm), been exhibited a novel class of materials with unusual electronic and optical properties, which was attributed to their exceptionally small thickness and large lateral dimensions.[6] The synthesized atomically flat II-VI NPLs (CdS, CdSe, and CdTe) with well-defined thickness (several monolayers) exhibit strong thickness-dependent optical and electronic properties due to 1D quantum confinement.[7] Regarding a fixed thickness of NPLs, their photoluminescence (PL) and absorption peaks are almost fixed and difficult to adjust. In addition, because of the atomically flat and extended surfaces, the 2D NPLs exhibit much narrower absorption and emission linewidths as compared to the best colloidal CdSe nanocrystallites ensembles.[7-12] Efros *et al.* recently mentioned that these colloidal NPLs may combine the best characteristics of both worlds: the wide tunability of the absorption and PL of NCs and the short decay time of exciton in quantum wells.[7]

High pressure is an effective approach to change the structures and properties of many materials, such as surface states, structural phases, electronic properties and shapes of NCs. NCs under high pressure have revealed many novel phenomena in recent years, including the effect of critical size of some NCs,[13-16] and the formation of novel 1D or 2D nanostructures and architectures by the pressure-induced orientation and attachment process,[17,18] as well as the phase transformation from metastable structure to stable structure of some NCs at elevated pressures.[19,20] In order to study the pressure-dependent band gap and optical properties of semiconductor NCs, the compressed NCs were mainly focused on 0D quantum dots (QDs).[21-24] In recent years, some other shaped-NCs such as core/shell structure,[25] rods, and tetrapods,[26] have also been investigated. However, there have been so far few reports on the pressure-dependent optical behaviors of the 2D crystalline NPLs.[27]

In this work, we systematically investigated the optical behavior, band gap modulation, crystalline stability, and carrier decay dynamics of CdSe NPLs with different thickness by using *in situ* high-pressure PL, absorption, and time-resolved PL spectroscopy. Our experimental results indicate that the pressure-induced optical and electronic properties of CdSe NPLs are strongly related to their unique geometric shape, crystalline stability and surface conditions, showing significant difference compared with other shaped CdSe NCs. In addition, high pressure could be used to modulate the band gap and optical properties of CdSe NPLs in a certain range, which is difficult to achieve under ambient conditions. Afterward, the difference of optical behavior under high pressure between CdSe NPLs and other shaped NCs is systematically discussed.

Experimental Section

Chemicals

Cadmium nitrate tetrahydrate ($Cd(NO_3)_2$•$4H_2O$, 98%), cadmium acetate dihydrate ($Cd(Ac)_2$•$2H_2O$, 98%) , zinc acetate ($Zn(Ac)_2$, 99.99%) 1-octadecene (ODE, 90%), sodium myristic (98%), selenium powder (99.5%) were all purchased from Sigma Aldrich.

Methanol, ethanol and hexane were obtained from commercial sources.

Synthesis of CdSe NPLs with Different Monolayers.

The synthetic procedure of CdSe NPLs with tuneable thicknesses adopted and modified from previously established approaches.[6,7]

Preparation of Cd(myristate)$_2$.

$Cd(NO_3)_2$•$4H_2O$ (1.23 g) and sodium myristic (3.13 g) are dissolved in 40 and 250 ml methanol respectively. These two clear solutions are mixed. The resulting white precipitate is filtered and washed by methanol for several times, and dried in an oven for 12 h at 50 ^oC.

Synthesis of 5-monolayer (5 ML) CdSe NPLs: 0.17 g (0.3 mmol) of Cd(myristate)$_2$ and 15 ml of ODE are loaded in a 50 ml three neck flask. The mixture is heated under stirring and N_2 flow at 120 ^oC for 30 minutes. After that, the mixture is heated to 240 ^oC and keep for several minutes. A Se solution containing 0.012 g (0.15 mmol) of Se and 1.0 ml ODE is swiftly injected. After 10 seconds, 0.12 g (0.45 mmol) of $Cd(Ac)_2$•$2H_2O$ was added into the flask. The mixture was heated for 10 minutes at 240 ^oC.

Synthesis of 4 ML CdSe NPLs: 0.17 g (0.3 mmol) of Cd(myristate)$_2$, 0.012 g (0.15 mmol) of Se and 15 ml of ODE are introduced in a three neck flask and string under N_2 flow at 120 ^oC for 30 minutes. After that, the mixture is heated to 195 ^oC and keep for several minutes, and then 0.055 g (0.3 mmol) of $Zn(Ac)_2$ is introduced. The mixture is then heated to 240 ^oC and kept for 10 minutes.

Synthesis of 3&4 and 4&5 ML CdSe NPLs: through adjusting the dosage of $Cd(Ac)_2$•$2H_2O$ and the reaction temperature, the samples of 3&4 and 4&5 ML CdSe NPLs could be synthesized by the same synthesis process mentioned above. The detailed experimental methods are described in Supplementary Information.

Characterization: A JEM-2200FS transmission electron microscope (TEM) operating at 200 kV was used to take TEM, high-resolution TEM (HRTEM) images and selected area electron diffraction (SAED) patterns. The phase purity of the obtained samples was characterized by X-ray powder diffraction (XRD, Shimadzu XRD-6000 working with a Cu – Kα target).

***In Situ* High-Pressure Experiments.**

The high pressure experiments shown in this paper were carried out using a symmetric diamond anvil cell (DAC) with type Ia ultra low-fluorescence diamonds. The diamonds culet sizes are 500 μm. A T301 stainless steel gasket was preindented by the diamonds and then drilled to produce a 200 μm diameter cavity for the sample. Typically, the prepared CdSe NPLs solution was dropped in the gasket hole together with several small ruby chips to determine the pressure using the standard ruby fluorescent technique.[28]

***In Situ* High-Pressure Optical Experiments.** CdSe NPLs PL spectra were recorded using modified spectrophotometer (Photon Technology International, Inc.). A semiconductor laser with 405 nm excitation wavelength was used for all fluorescence studies. PL decay curves were obtained by using a High Resolution Nitrogen and Dye Laser (PTI, Inc.) as the excitation source (λ_{exc}=481 nm, 800 ps pulse width, 10 Hz repetition rate). NPLs absorption spectra were recorded by an optical fibber spectrometer (Ocean Optics, QE65000).

***In Situ* Angle-Dispersive Synchrotron XRD Experiments.** The measurements were performed at beamline X17C in the national synchrotron light source (NSLS) at Brookhaven National Laboratory. The X-ray beam had a wavelength of 0.4066 Å. The diffraction data were collected using MAR165 CCD detector and subsequently performed with the software FIT2D to obtain 2D images.

Results and Discussion.

TEM images of the obtained 5 ML thickness CdSe NPLs exhibited to be rectangular with lateral dimensions ranging from 30 nm to several hundred nanometres (Figure 1a, b). A clear and continuous lattice fringe can be observed in the HRTEM image, indicating that these resulting NPLs have a single-crystalline structure (Figure 1c). The distance between neighbouring fringes was measured to be 0.23 nm, close to the (220) lattice spacing of zinc blende (ZB) CdSe. The side view HRTEM image (Figure 1d) with "standing up" NPLs verified the thickness of ~2.1 nm, in good accordance with 5 ML CdSe NPLs proposed in other works.[7] Figure 1e presented the XRD

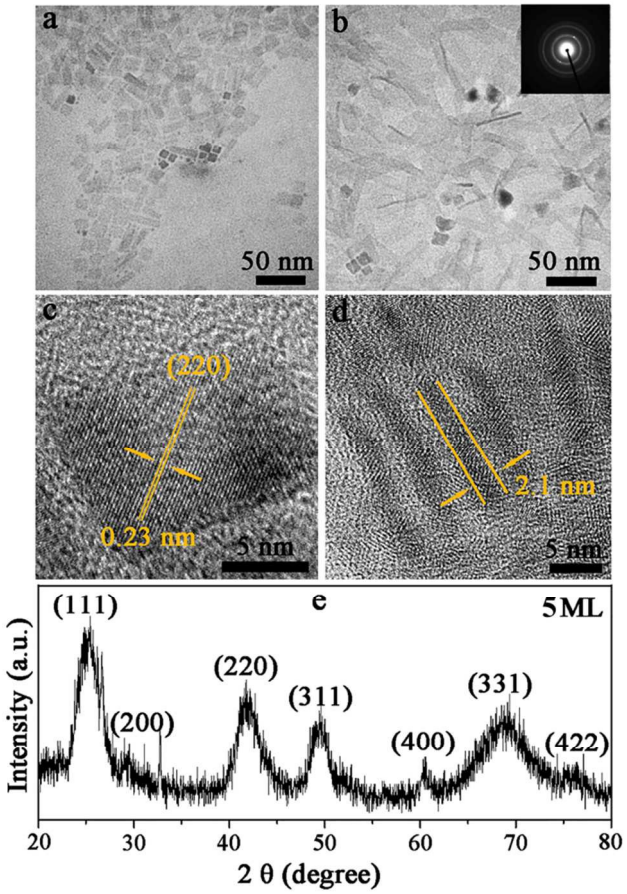

Figure 1. Basic characterization of 5 ML CdSe NPLs. (a, b) TEM images of CdSe NPLs with different shape and lateral dimensions. The inset in Figure b shows the corresponding SAED pattern. (c) HRTEM image of CdSe NPLs. (d) HRTEM image of side view of CdSe NPLs. (e) XRD pattern of corresponding CdSe NPLs.

patterns of the related CdSe NPLs. All the diffraction peaks were labelled and could be indexed to ZB crystal structure.

The optical properties of the resulting products are shown in Figure 2. Under ambient conditions, the CdSe NPLs exhibit a strict thickness-dependent absorption and emission spectra. The extracted Lorentz linewidths of these CdSe NPLs exhibit a typical quantum well property: the heavy-hole (hh)-transitions are much narrower than the light-hole (lh)-transitions (Figure 2a) due to the different band curvatures at the Γ point, which is attribute to different effective masses and density of states.[7] The emission spectra for each NPLs population have very narrow full width half-maximums (FWHM), and there is no significant Stokes shift between emission and absorption spectra, in contrast with the large Stokes shifts observed from other shaped CdSe NCs. Moreover, except for the synthesis of thickness-fixed NPLs (*e.g.* pure 5 ML NPL sample), CdSe NPLs samples containing two different thicknesses (*e.g.* 3&4, 4&5 ML) could also be prepared by changing the reaction temperature and the injected dosage of salt acetate (Figure 2b). The optical results and TEM images of these obtained CdSe NPLs imply that the lateral dimensions have only little influence on their absorption and emission spectra.

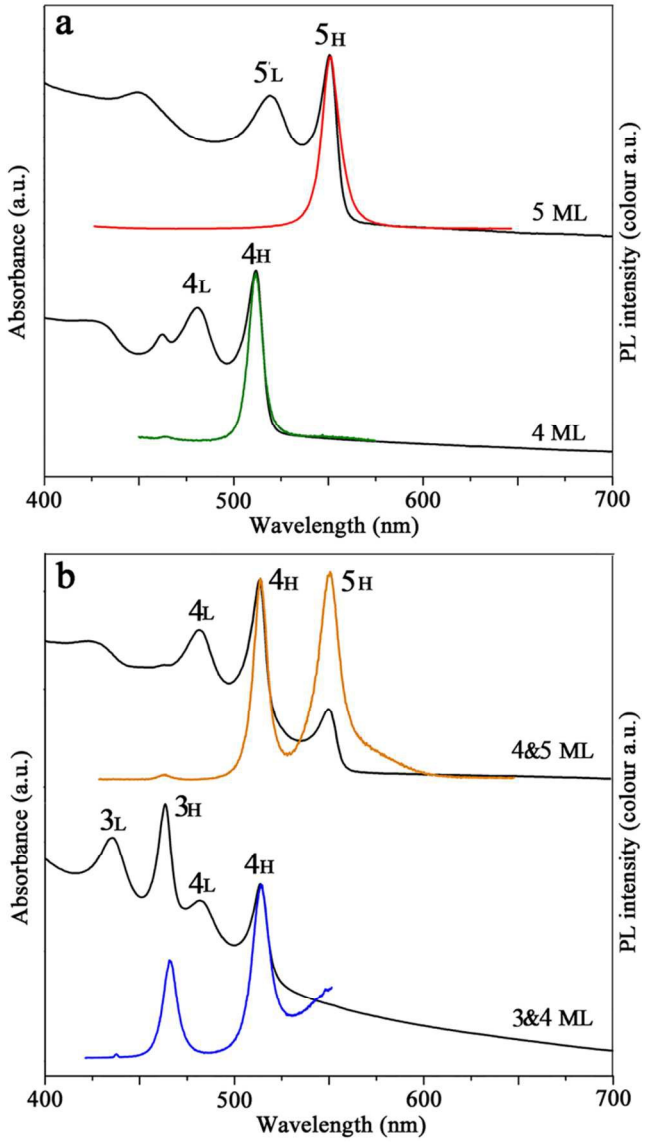

Figure 2. PL and absorption spectra of different thicknesses CdSe NPLs. (a) Pure 4 ML and 5 ML CdSe NPLs. (b) Contains two different thicknesses of CdSe NPLs samples.

The pressure-dependent PL spectra of pure 4 and 5 ML CdSe NPLs samples in a silicone fluid pressure medium are shown in Figure 3. As the external pressure is applied, both PL peaks of 4 and 5 ML NPLs shift monotonically toward lower wavelength in a narrow range of wavelength (~11 and ~7 nm; ~0.053 and ~0.041 eV), until increasing pressure up to ~2.0 and 1.8 GPa, respectively. And then, these PL peaks begin to shift toward higher wavelength slowly with further increasing pressure, and show a marked broadening of the PL spectra, which is caused by the stress-strain induced decrease of lattice symmetry and structure order. Finally, the PL of 4 and 5 ML CdSe NPLs disappeared when the pressure approached to a critical value of around 7.7 and 7.2 GPa respectively. In addition, an anomalous and irreversible optical phenomenon of CdSe NPLs could be observed during the release of pressure (red lines shown in Figure 3). In order to avoid contingency of the anomalous phenomenon mentioned above, we further examined the similar experimental processes repeatedly under diverse conditions using different CdSe NPLs samples (Figure S1-S6). The same anomalous phenomenon could also be observed (the detailed experimental methods and results are described in Supplementary Information).

The pressure-induced PL peak position shifts of pure 4 and 5 ML CdSe NPLs samples mentioned above are summarized in Figure 4. Depending on the different thicknesses of NPLs, several rules could be obtained. First, the PL peaks exhibit blue shifts under lower pressures and then continuously shift towards high wavelength until disappeared. Second, the critical pressure for the PL disappearance of 4 ML NPLs is a little higher than that of 5 ML NPLs, which is similar with size dependence pressure of phase transformation of CdSe QDs. Third, the disappeared PL of different thicknesses of NPLs under high pressure cannot restore to their original states after

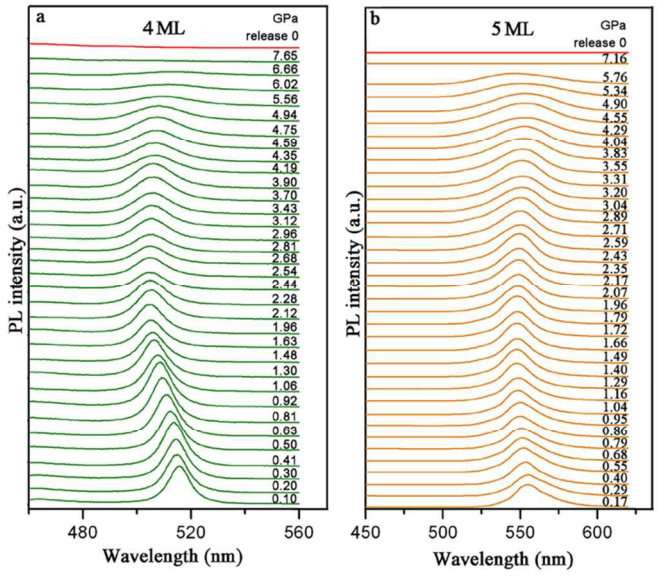

Figure 3. Pressure-dependent PL spectra of CdSe NPLs in silicone fluid pressure medium. (a) 4 ML CdSe NPLs; (b) 5 ML CdSe NPLs. The red spectral lines are corresponding recovered PL spectra, respectively.

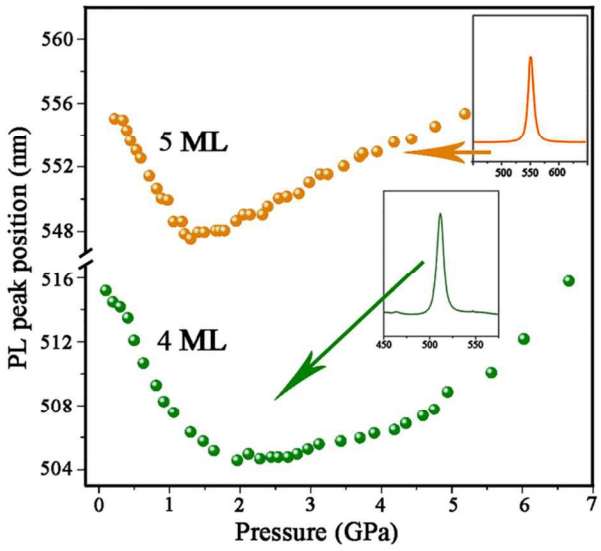

Figure 4. Pressure dependence PL peak positions of 4 and 5 ML CdSe NPLs.

releasing pressure, which is greatly different from other shaped CdSe nanostructures (Figure S7).

About other shaped CdSe NCs, both synchrotron X-ray diffraction and optical spectroscopy measurements indicated that these CdSe NCs exhibit reversible changes in both structure and optical spectra under high pressure.[21, 29, 30] Therefore, an important question is what changes happened of CdSe NPLs under high pressure? Figure 5 shows several representative XRD patterns of 5 ML CdSe NPLs during compression and decompression processes collected under a pressure cycle of 0-9.6 GPa, respectively. At ambient pressure, the diffraction rings indicated that 5 ML CdSe NPLs crystallize in a ZB structure. The ZB structure of NPLs remained stable in the lower pressure range (*e.g.* 2.2 GPa, Figure 5b). After the pressure increased to 9.6 GPa, new diffraction rings pattern of rock salt (RS) structure could be observed (Figure 5c), indicating the finish of phase transition. Upon releasing the pressure, the high pressure RS phase remains stable down to ~1.3 GPa (Figure 5d). With further reduction of pressure to ambient conditions, the diffraction patterns turn to the original ZB phase, indicating a reversible process of structural phase transition (Figure 5e). From a more intuitive point of view, TEM and HRTEM images of the retrieved samples indicated that the high pressure treated samples not only exhibit the similar morphology but also have the same crystal structure compared with the uncompressed 5 ML NPLs (Figure 5f, 5g, S8). In addition, a large scale assembly by stacking could also be observed from low magnification TEM images (Figure S6), which show the similar results compared with Dubertret group's work.[10]

Obviously, the disappeared PL of pressure treated NPLs were not attributed to the irreversible structure transformation. For the quenching of the PL of CdSe NCs under ambient pressure, surface tailoring in studying NCs-ligand bonding has great influence on the optical properties.[31,32] Through a ligand-exchange process (*e.g.* mercaptopropionic acid, pyridine, or thiolates), these ligands act as surface hole traps which lead to quench the PL of semiconductor NCs. In addition, this ligand-exchange process could cause surface atoms to remove from the NCs surface, the NCs shall experience some abrupt changes of the optical properties at the interface. Meanwhile, Wang and co-workers[33] have found that the

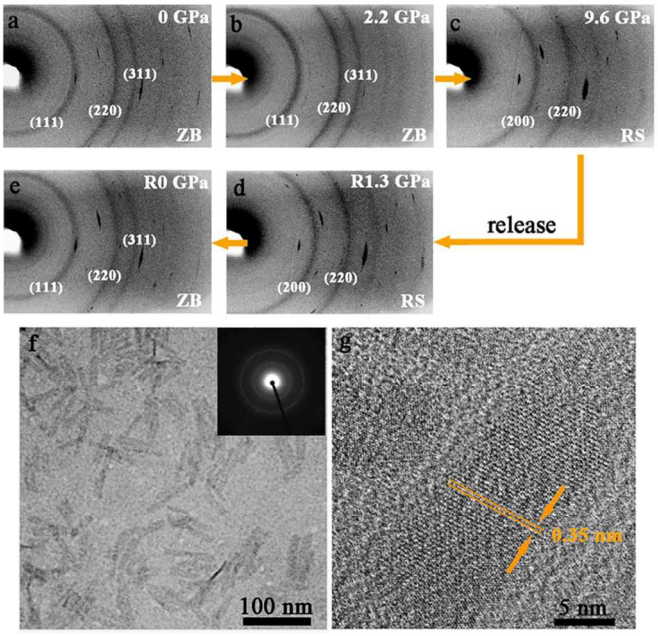

Figure 5. Raw diffraction data obtained on 5 ML CdSe NPLs under high pressure. (a-c) compression; (d, e) release. (f) TEM image of 5 ML NPLs after decompression from 9.6 GPa. (g) HRTEM image of corresponding sample after pressure release. The inset in Figure f is corresponding selected area electron diffraction pattern.

enhancement of structural stability and elastic strength of lamellar CdSe nanosheets can be correlated with the presence of surface-bonded soft organic ligands. These study results indicate that organic ligands play an important role in the structure and optical properties of CdSe NCs. Compared with spherical CdSe QDs, the capping ligands of NPLs were mainly concentrated on the two lateral surfaces because of the exceptionally small thickness and large lateral dimensions. Therefore, we infer that CdSe NPLs-ligand bonding can easily undergo an abrupt process via high pressure treatment, which gives rise to the occurrence of NPLs surface atoms relaxation, reconstruction and/or removal. The subtle changes of NPLs-ligand bonding lead the photo generated holes to be trapped and quench the PL of NPLs. In addition, with the pressure increasing, samples tend to minimize their volume. Assembly by stacking is an efficient way for NPLs with large lateral size and small uniform thickness (Figure S6). Moreover, considering the interaction between two NCs with ligands bound on their surface, the self-assembly of 2D NPLs is far more effective than other shaped NCs. When two plate-like NCs are brought together, all the ligands on one face of one particle come in close contact with all the ligands on the opposing face of the other. On the contrary, when spherical or other shaped NCs approach, only a small fraction of the capping ligands could interact.[10] The stacking of NPLs significantly increases the nonradioactive recombination rate, due to the efficient exciton migration among the NPLs *via* homo Förster resonance energy transfer.[34] In contrast, when the employed pressure is lower than the critical pressure, these subtle changes could not generate, and corresponding optical behaviours show a reversible process (Figure S4a, 4b).

We further investigated the pressure-dependent optical absorption of 4 and 5 ML NPLs mixed with silicone fluid pressure medium respectively. Under high pressure, the first excitonic absorption peaks (electron/hh-transition) of both 4 and 5 ML NPLs shift towards lower wavelength, and corresponding peak positions shift

about 10 nm (ΔE=0.048 eV) at about 1.8 and 2.0 GPa, respectively (Figure 6). Further increasing the pressure, a marked red shift tendency can be observed (Figure 6c and d). The first excitonic absorption peaks of 4 and 5 ML NPLs disappear, when the pressures are enhanced to 7.2 and 6.9 GPa, respectively. In contrast, the absorption peaks related to the electron/lh-transition exhibit continuous and faster blue shift than electron/hh-transition under high pressure. Similar with PL spectra, these absorption spectra undergo an irreversible process after releasing pressure, which is in good agreement with irreversible PL spectra as mentioned above.

For the CdSe QDs, a blue shift of the PL and absorption peak position with increasing pressure could be observed due to pressure-induced contraction of the crystallattice.[35] Similarly, in quasi-2D NPLs, the strength of exciton coupling with emitted photons was affected by the thickness of NPLs. Under ambient conditions, the hh energy is connected with the width between quantum wells, $E_{hh} \propto (1/L_z^2)$. Therefore, the trend of tiny blue shift of PL and absorption spectra was mainly caused by the compression of the crystal lattice, which slightly decreases the thickness and narrow the quantum well of NPLs under high pressure. Under ambient conditions, as the thickness of NPLs decreases, the blue shift speed of the electron/lh transitions is usually faster than that of the electron/hh transition, which could be connected with a strong non-parabolicity of the lh energy spectra appearing in a strong-confinement regime by analysing the band-edge dispersion of the hole spectra in the vicinity of the Γ point of the Brillouin zone.[7] In other word, more and more significant Stokes shift between PL and absorption spectra, as well as the spacing between electron/lh transitions and electron/hh transition can be observed with decreasing the thickness of II-VI semiconductor NPLs. Therefore, the similar reason could be used to explain the behavior of the pressure-depended absorption spectra shown in Figure 6c and d. With the thickness of CdSe NPLs decrease caused by contraction of the crystal lattice under high pressure, the blue shift of the electron/lh transitions is faster than the electron/hh transition, causing the spacing increase.

In addition, both pressure-dependent PL and absorption spectra of these CdSe NPLs exhibit noteworthy red shift tendency after the initial blue shift. These phenomena might be caused by several reasonable reasons. (1) Pressure-induced intermediate phase (*e.g. h*-MgO) causes optical spectra showing red shift;[36] (2) pressure caused capping ligand and surface atoms reconstruction, which lead the dielectric environment of CdSe NPLs to change, induced tremendous influence on the binding energies;[8,37-39] (3) pressure media and compression environment induced peaks of PL and absorption to display red shift.[40] Among these potential reasons, we think the changing of dielectric environment of compressed system might play the dominant role.

Under ambient conditions, the thickness *Lz* of these quasi-two-dimensional CdSe NPLs is smaller than the Bohr radius (~6 nm). Therefore, the optical property is mainly determined by 1D-confined energy levels. The lowest level of the hh energy in the NPLs is given by eight-band model as follow: [7, 38]

$$E_{hh} = -(\gamma_1 - 2\gamma_2)\frac{\hbar^2\pi^2}{2m_e L_z^2} \quad (1)$$

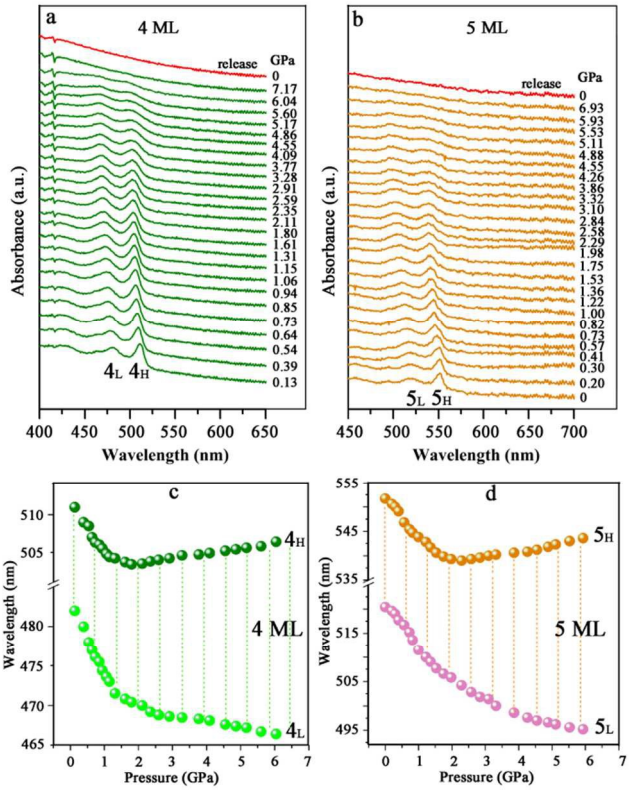

Figure 6. Absorption spectra of CdSe NPLs as a function of pressure. (a) 4 ML; (b) 5 ML. The red spectral lines are corresponding recovered absorption spectra, respectively. (c, d) wavelength of the electron/lh-transition (light green and pink) and electron/hh-transition (dark green and orange) transitions of 4 and 5 ML CdSe NPLs versus the pressure, respectively.

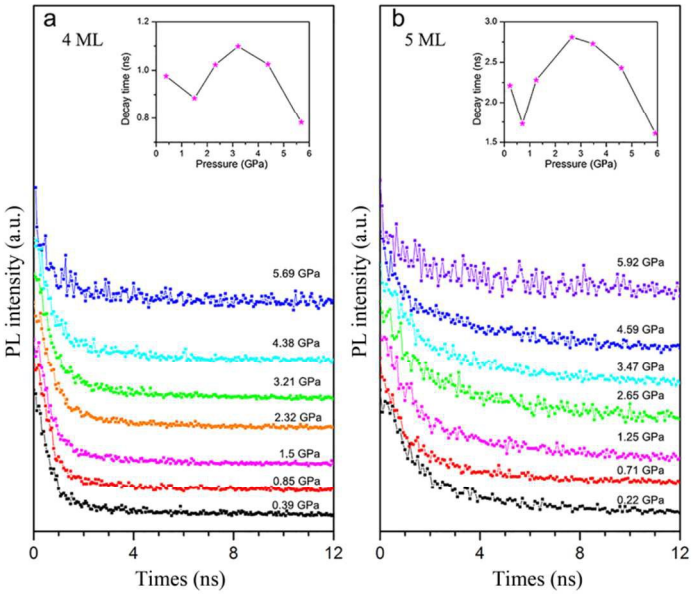

Figure 7. Pressure-dependent PL decay curves of different thick CdSe NPLs. (a) 4 ML CdSe NPLs; (b) 5 ML CdSe NPLs. The insets show the corresponding average PL decay times as a function of pressure.

Where m_e is the electron mass, and γ_1, γ_2 is the Luttinger_Kohn parameters of the valence band. Due to NPLs surrounded by an infinite potential barrier, $\hbar^2\pi^2/2m_eL_z^2$ is the kinetic energy of a free electron. The optical transition energies between the ground electron and the hh transition can be written as: [7, 38]

$$E_{hhe} = E_e - E_{hh} - E_{bhh} \quad (2)$$

Where E_{bhh} is the binding energy of the two-dimensional electron/hh exciton and its value is very sensitive to dielectric environment.

Under high pressure, there is an initial sharp decrease in volume of CdSe NPLs between 0 GPa and 2.5 GPa examined by Wang et.al.[29] The compression on thickness of CdSe NPLs play the dominant effect, because the quantization energy grows as $1/{L_z}^2$. This caused optical transition energies (E_{hhe}) of CdSe NPLs to increase, resulting in a blue shift tendency of PL and absorption (electron/hh-transition) peaks under low pressure range. With pressure further increased, the volume decrease of CdSe NPLs becomes significantly slowly.[33] In contrast, the pressure induced change of dielectric environment, solidification and crystallization of the ligand, and reconstruction/removal of the NPLs' surface atoms, made the binding energy E_{bhh} grow much faster than quantization energy ($\hbar^2\pi^2/2m_eL_z^2$). This lead optical transition energies (E_{hhe}) to decrease, resulting in a red shift tendency of PL and absorption (electron/hh-transition) peaks under higher pressure.

Compared with spherical CdSe QDs, the significant shortened fluorescence decay time of NPLs could be observed. Siebbeles *et al*. [41] confirmed that the electron and holes of CdSe NPLs are bound in the form of neutral excitons, while the fraction of free charges is much smaller. The biexciton Auger recombination rate in NPLs is more than 1 order of magnitude smaller than QDs of equal volume, which caused NPLs to exhibit fast excitonic decay times. Figure 7 shows the pressure-dependent time-resolved PL spectroscopy of 4 and 5 ML CdSe NPLs. We found that the decay time of 4 ML NPLs is shorter than 5 ML at atmosphere pressure. The insets in Figure 7 summarize the averaged fluorescence decay time as a function of pressure. Through third-order expontail fitting process (Table S1, S2), we can find that the decay time of both 4 and 5 ML CdSe NPLs exhibit the similar transformation processes. With increasing pressure from 0 to ~1.0 GPa, the decay time of CdSe NPLs PL exhibit a little decrease, which was caused by crystal lattice shrink and blue shift of PL peak position. When the pressure further increased to ~3.0 GPa, the decay time tend to increase. Meanwhile, both PL and absorption of CdSe NPLs exhibit red shift trend, indicating that oscillator strength of the radiation is reduced. This might be caused by the applied stress in the crystal reducing the electron-hole wave function overlap possibly due to a created internal field. When the applied pressure exceeds ~3.0 GPa, the decay time of PL exhibit decrease process again. This process might be attributed to the reconstruction and removal of ligand, and these phenomena was occurred at lower pressure than ~3.0 GPa. And this changing tendency plays the dominant role to effect their decay time when pressure is above ~3.0 GPa. Both the increase of binding energy and the removal of ligand accelerate the combination of holes and exactions, which play a significant role for non-radiative recombination.[9,34] But overall, the pressure-depended PL decay time exhibit minor change ranges under high pressure (<1.5 ns). The small range of variation of PL decay time is in good agreement with corresponding tiny change of PL peak position under high pressure.

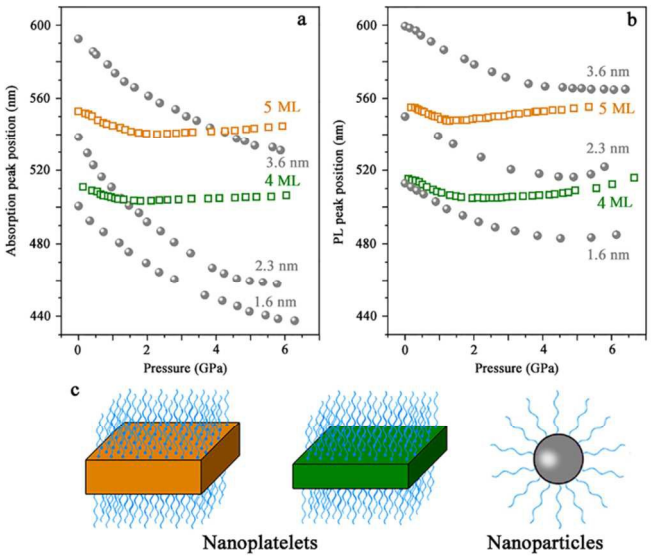

Figure 8. Morphology- and size-dependent optical behaviors of CdSe NCs under high pressure. (a) Pressure-dependent absorption spectra; (b) pressure-dependent PL spectra; (c) schematic drawing of the CdSe NPLs and QDs.

Under ambient conditions, the optical properties already exhibit some differences between CdSe NPLs and QDs. Under high pressure,the pressure-dependent optical behaviors also show significant discrepancies. In order to better understand the differences, both pressure-induced absorption and PL behaviors of CdSe NPLs and QDs were summarized in Figure 8. CdSe QDs with tuneable particle sizes were synthesized by according to previously established approaches (the detailed experimental methods are described inSupplementary Information).[42] We selected three different sizes of CdSe QDs (~3.6, 2.3, and 1.6 nm) for performing high pressure optical experiments with silicone fluid as pressure medium. The first excitonic absorption peaks of these CdSe QDs exhibit a continuous blue shift with increasing pressure, until PL disappears completely (Figure 8a). The peak position could shift in a wide range of wavelengths (> 60 nm, ΔE > 0.27 eV). The position of the first excitonic absorption peaks can be fitted by a quadratic function E_{Ab} (P) = E_0+αP+ βP^2, where α and β are pressure coefficients of linear and quadratic terms. Similarly, corresponding pressure-dependent PL spectra exhibit the similar behavior (Figure 8b).

For the CdSe NPLs, both their absorption (electron/hh-transition) and PL peak positions could only shift in a narrow range of wavelength (<15 nm, ΔE<0.053 eV) under high pressure. In addition, these experimental data points neither satisfied the linear nor the quadratic equation. The caused great differences between QDs and NPLs could be attributed to two reasonable aspects (Figure 8c). One aspect is their unique morphologies; the other is morphology-dependent surface ligands bonding. For the 2D CdSe NPLs, the ground quantum size level of electrons, lh and hh are limited to the very narrow quantum well created by the NPLs.[7] Recently, Achtstein *et al.* demonstrated that the 2D hh-exciton states of ZB-CdSe NPLs exhibit a strong influence of vertical confinement and dielectric screening.[8] On the other hand, Wang *et al*. have investigated that the transformation pressure of CdSe NPLs is much higher than bulk CdSe crystal by the experiments of small and wide-angle X-ray diffraction images under high pressure. They found that the soft ligands not only increase the stability of NPLs, but also improve its elastic strength and fracture toughness.[29] Therefore,

based on their unique 2D morphologies and capping ligands-induced structural stability, the optical properties of CdSe NPLs exhibit remarkable difference compared with other shaped NCs, whether under atmospheric or high pressure condition.

Conclusions

In summary, we have investigated the optical behavior, band gap energy modulation, crystalline stability, and carrier decay dynamics of CdSe NPLs with different thicknesses under high pressure. Several significant differences of pressure-induced optical properties of CdSe NPLs could be observed in contrast to other shaped NCs. These peculiar phenomena are attributed to their unique geometric shapes and distinctive surface soft ligand bonding. In addition, under ambient conditions, the PL and absorption peak energies of CdSe NPLs are almost fixed, and only depend on the number of atomically flat surfaces. However, high pressure could be used to modulate their band gap energies in a certain range, which is difficult to achieve under atmospheres. The results of current work enrich the high pressure research of shape-depended CdSe material.

Acknowledgements

We highly appreciate Prof. Dr. Bo Zou for the partial fund support and the help of *in situ* high pressure PL and absorption spectra measurements. This work was supported by NSFC (Nos. 91227202, 51102108, 11204101 and 11404135), RFDP (No. 20120061130006), China Postdoctoral Science Foundation (Nos. 2012M511336, 2013T60326, 2012M511327, 2014M550171 and 2014M561281) and the National Basic Research Program of China (No. 2011CB808200), and Jilin Provincial Science & Technology Development Program (No. 20150520087JH).

Notes

[a] State Key Laboratory of Superhard Materials, Jilin University, Changchun, 130012, P. R. China

* Correspondence and requests for materials should be addressed to Y.W. (email: ynwang@jlu.edu.cn), K.W. (email: kaiwang@jlu.edu.cn).

References

1 X. G. Peng, L. Manna, W. D. Yang, J. Wickham, E. Scher, A. Kadavanich, A. P. Alivisators, *Nature,* 2000, ***404***, 59-61.
2 G. J. Xiao, Y. Zeng, Y. Y. Jiang, J. J. Ning, W. T. Zheng, B. B. Liu, X. D. Chen, G. T. Zou, B. Zou, *small,* 2013, ***9***, 793-799.
3 G. J. Xiao, C. Y. Zhu, Y. M. Ma, B. B. Liu, G. T. Zou, B, Zou, *Angew. Chem. Int. Ed.,* 2014, ***53***, 729 -733.
4 J. J. Ning, K. K. Men, G. J. Xiao, L. Wang, Q. Q. Dai, B. Zou, B. B. Liu, G. T. Zou, *Nanoscale,* 2010, ***2***, 1699-1703.
5 G. J. Xiao, Y. N. Wang, J. J. Ning, Y. J. Wei, B. B. Liu, W. W. Yu, G. T. Zou, B. Zou, *RSC Adv.,* 2013, ***3***, 8104-8130.
6 S. Ithurria, B. Dubertret, *J. Am. Chem. Soc*., 2008, ***130***, 16504-16505.
7 S. Ithurria, M. D. Tessier, B. Mahler, R. P. S. M. Lobo, B. Dubertret, AI. L. Efros, *Nat. Mater.,* 2011, ***10***, 936-941.
8 A. W. Achtstein, A. Schliwa, A. Prudnikau, M. Hardzei, M. V. Artemyev, C. Thomsen, U. Woggon, *Nano Lett*., 2012, ***12***, 3151-3157.
9 C. She, I. Fedin, D. S. Dolzhnikov, A. Demortiere, R. D. Schaller, M. Pelton, D. V. Talapin, *Nano Lett*., 2014, ***14***, 2772-2777.
10 B. Abecassis, M. D. Tessier, P. Davidson, B. Dubertret, *Nano Lett*., 2014, ***14***, 710-715.
11 L. T. Kunneman, J. M. Schins,S. Pedetti, H. Heuclin, F. C. Grozema, A. J. Houtepen, B. Dubertret , L. D. A. Siebbeles, *Nano Lett*., 2014, ***14***, 7039-7045.
12 B. Guzelturk, M. Olutas, S. Delikanli, Y. Kelestemur, O. Erdem, H. V. Demir, *Nanoscale*, 2015, *7*, 2345-2351.
13 L. Wang, W. G. Yang, Y. Ding, Y. Ren, S. G. Xiao, B. B. Liu, S. V. Sinogeikin, Y. Meng, D. J. Gosztola, G. Y. Shen, R. J. Hemley, W. L. Mao, H. G. Mao, *Phys. Rev. Lett*., 2010, ***105***, 095701.
14 Z. W. Quan, Y. X. Wang, I. T. Bae, W. S. Loc, C. Y. Wang, Z. W. Wang, J. Y. Fang, *Nano Lett*., 2011, ***11***, 5531-5536.
15 V. Swamy, A. Kuznetsov, L. S. Dubrovinsky, P. F. McMillan, V. B. Prakapenka, G. Shen, B. C. Muddle, *Phys. Rev. Lett*., 2006, ***96***, 135702.
16 H. S. Yuan, K. Wang, S. R. Li, X. Tan, Q. Li, T. T. Yan, B. Y. Cheng, K. Yang, B. B. Liu, G. T. Zou, B. Zou, *J. Phys. Chem. C,* 2012, ***116***, 24837−24844.
17 H. M. Wu, F. Bai, Z. C. Sun, R. E. Haddad, D. M. Boye, Z. W. Wang, J. Y. Huang, H. Y. Fan, *J. Am. Chem. Soc*., 2010, ***132***, 12826-12828.
18 Z. W. Wang, C. Schliehe, T. Wang, Y. Nagaoka, Y. C. Cao, W. A. Bassett, H. M. Wu, H. Y. Fan, *J. Am. Chem. Soc*., 2011, ***133***, 14484-14487.
19 X. Y. Yang, Y. N. Wang, K. Wang, Y. M. Sui, M. G. Zhang, B. Li, Y. M. Ma, B. B. Liu, G. T. Zou, B. Zou, *J. Phys. Chem. C,* 2012, ***116***, 3292-3297.
20 N. R. Xiao, L. Zhu, K. Wang, Q. Q. Dai, Y. N. Wang, S. R. Li, Y. M. Sui, Y. M. Ma, J. Liu, B. B. Liu, G. T. Zou, B. Zou, *Nanoscale*, 2012, ***4***, 7443-7447.
21 S. H. Tolbert, A. P. Alivisatos, *J. Chem. Phys*., 1995, ***102***, 4642-4656.
22 Y. C. Lin, W. C. Chou, A. S. Susha, S. V. Kershaw, A. L.Rogach, *Nanoscale*, 2013, ***5***, 3400-3405.
23 J. M. Pietryga, K. K. Zhuravlev, M. Whitehead, V. I. Klimov, R. D. Schaller, *Phys. Rev. Lett*., 2008, ***101***, 217401.
24 C. S. Menoni, L. Miao, D. Patel, O. I. Mic'ic', A. J. Nozik, *Phys. Rev. Lett*., 2000, ***84***, 4168-4171.
25 H. M. Fan, Z. H. Ni, Y. P. Feng, X. F. Fan, J. L. Kuo, Z. X. Shen, B. S. Zou, *Appl. Phys. Lett*., 2007, ***90***, 021921.
26 C. L. Choi, K. J. Koski, S. Sivasankar, A. P. Alivisatos, *Nano Lett*., 2009, ***9***, 3544-3549.
27 X. M. Dou, K. Ding, D. S. Jiang, B. Q. Sun, *ACS Nan*o, 2014, ***8 (7)***, 7458–7464
28 H. K. Mao, J. Xu, P. M. Bell, *J. Geophys. Res*., 1986, ***91***, 4673-4676.
29 S. H. Tolbert, A. P. Alivisatos, *Science,* 1994, ***265***, 373-376.
30 Z. W. Wang, K. Finkelstein, C. Ma, Z. L. Wang, *Appl. Phys. Lett*., 2007, ***90***, 113115.
31 X. H. Ji, D. Copenhaver, C. Sichmeller, X. G. Peng, *J. Am. Chem. Soc*., 2008, ***130***, 5726-5735.
32 B. Blackman, D. Battaglia, X. G. Peng, *Chem. Mater.,* 2008, ***20***, 4847-4853.
33 Z. W. Wang, X. D. Wen, R. Hoffmann, J. S. Son, R. Li, C. C. Fang, D. M. Smilgies, T. Hyeon, *Proc. Natl. Acad. Sci. U. S. A.,* 2010, ***107***, 17119-17124.
34 B. Guzelturk, O. Erdem, M. Olutas, Y. Kelestemur, H.V. Demir, *ACS Nano,* 2014, ***8***, 12524-12533.

35 X. L. Li, B. B. Liu, Z. P. Li, Q. J. Li, Y. G. Zou, D. D. Liu, D. M. Li, B. Zou, T. Cui, G. T. Zou, *J. Phys. Chem. C,* 2009, ***113***, 4737-4740.
36 M. Grünwald, E. Rabani, C. Dellago, *Phys. Rev. Lett*., 2006, ***96***, 255701.
37 R. W. Meulenberg, G. F. Strouse. *Phys. Rev. B* 2002, ***66***, 035317.
38 Al. L. Efros, M. Rosen, *Annu. Rev. Mater. Sci*., 2000, ***30***, 475-521.
39 A. Franceschetti, A. Williamson, A. Zunger, *J. Phys. Chem. B,* 2000, ***104***, 3398-3401.
40 C. D. Grant, J. C. Crowhurst, S. Hamel, A. J. Williamson, N. Zaitseva, *Small,* 2008, ***4***, 788-794.
41 L. T. Kunneman, M. D. Tessier, H. Heuclin, B. Dubertret, Y. V. Aulin, F. C. Grozema, J. M. Schins, L. A. Siebbeles. *J. Phys. Chem. Lett*., 2013, ***4***, 3574-3578.
42 Q. Q. Dai, D. M. Li, H. Y. Chen, S. H. Kan, H. D. Li, S. Y. Gao, Y. Y. Hou, B. B. Liu, G. T. Zou, *J. Phys. Chem. B,* 2006, ***110***, 16508-16513.

NANOSCALE RSCPublishing

ARTICLE

TOC image

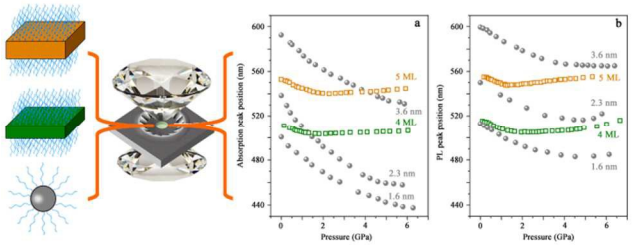

The optical properties of CdSe NPLs exhibit remarkable difference compared with other shaped CdSe NCs under high pressure.